

Quantum Monte Carlo study on the structures and energetics of cyclic and linear carbon clusters C_n ($n = 1, \dots, 10$)

B. G. A. Brito,¹ G.-Q. Hai,² and Ladir Cândido³

¹*Departamento de Física, Instituto de Ciências Exatas e Naturais e Educação (ICENE), Universidade Federal do Triângulo Mineiro–UFTM, 38064-200, Uberaba, Minas Gerais, Brazil*

²*Instituto de Física de São Carlos, Universidade de São Paulo, 13560-970, São Carlos, São Paulo, Brazil*

³*Instituto de Física, Universidade Federal de Goiás, 74001-970, Goiânia, Goiás, Brazil*



(Received 21 September 2018; published 12 December 2018)

Using fixed-node diffusion quantum Monte Carlo (DMC) simulation we investigate the structural properties and energetics of the linear and cyclic carbon clusters C_n for $n \leq 10$. We calculate the binding energy, the electron correlation energy, the dissociation energy, and the second difference in energy. We also present an analysis of the structural properties of the clusters. It is found that the bond lengths, binding energies, and dissociation energies obtained from the DMC calculations are in excellent agreement with the available experimental results. The electron-correlation contribution to the binding energy indicates that in the case of the linear isomers, the clusters of odd-number size are relatively more favored than their neighbors of even-number size, whereas for the cyclic isomers, we do not observe the oscillation pattern. In the range of cluster size under investigation, we find that the electron-correlation impact in the binding energy of the cyclic clusters is larger than that of the corresponding linear ones, varying from 30% to 40% of the binding energy values. The electron correlation is also essential to the stability of the clusters enhancing by up to 52% their dissociation energy. A comparative analysis of the dissociation energy and second difference in energy indicates that the linear isomers C_3 and C_5 are the most stable ones.

DOI: [10.1103/PhysRevA.98.062508](https://doi.org/10.1103/PhysRevA.98.062508)

I. INTRODUCTION

The discovery of the remarkable stability of the C_{60} fullerene and the development of fullerene chemistry have motivated both experimental and theoretical studies on carbon clusters over the last decades [1–3]. Small carbon clusters are present in a variety of astrophysical objects and in hydrocarbon flames [1,2]. Compounds based on small carbon clusters such as hydrocarbon or organometallic clusters have important applications in different areas [4]. Details of physical and chemical properties of carbon clusters are important for understanding a large variety of chemical systems [1,5]. The carbon compounds were the first system in which were observed planar structures with high stability, delocalized electrons, and symmetrical arrangement. These effects are directly related to the aromaticity, a fundamental concept of great importance for theoretical chemistry [6]. Recently, magnetic properties in carbon nanostructures have been reported for possible applications in spintronics, molecular magnetism, and spin functional nanodevices [7–10]. These magnetic properties have been considered interesting due to the orbital characteristic of the valence electrons in the carbon compounds [11].

Although there are many experimental and theoretical studies involving carbon clusters, some fundamental physical properties of small carbon clusters are not yet fully understood. The main difficulties in the theoretical investigations are how to include and correctly interpret the electron-correlation effects in these clusters. Quantum Monte Carlo (QMC) calculations have shown that important effects arise

when electron correlations are fully taken into account. Recently, the QMC method has been used in the study of structure and stability of carbon-cluster isomers such as ring, bowl, and cage structures for different cluster sizes [12–15]. These studies have shown the importance of including correctly the electron correlation contribution for estimation of the lower energy isomers in carbon clusters. The QMC method has shown good accuracy in the calculation of the energy of the metal clusters and the correct determination of quantities associated with the energy [16–21]. However, to the best of our knowledge, no investigations have been reported on the electron-correlation effects in the small carbon clusters on the quantities directly related to cluster stability such as the binding energy, dissociation energy, and second difference in energy.

In this paper, we study some energy-related properties of the small carbon clusters in order to understand better the electron-correlation effects on their structures and energetics. We use the fixed-node diffusion quantum Monte Carlo (DMC) simulation to provide an accurate evaluation of the ground-state energy and to estimate the correlation energy in the linear and cyclic isomers of the carbon clusters with up to 10 atoms. The paper is organized as follows. In Sec. II, we present the computational details and theoretical approaches for determination of the atomic structure and calculations of the total energy. The general results for the atomic structure, the ground-state energy, binding energy, second difference in energy, and dissociation energy are given in Sec. III. In this section, we also discuss the contribution of the electron

correlation to these quantities, and consequently to the stability of the clusters. The conclusions are given in Sec. IV.

II. COMPUTATIONAL DETAILS AND THEORETICAL APPROACHES

We use density functional theory (DFT), the Hartree-Fock (HF) approximation, and quantum Monte Carlo (QMC) simulation to investigate the structural properties and the energetics of the carbon clusters C_n . The atomic structure is determined by performing DFT calculation considering all electrons with exchange-correlation potential estimated within the generalized gradient approximation (GGA) by using the three-parameter hybrid exchange functional of Becke [22], the nonlocal correlation functional of Lee, Yang, and Parr (LYP) [23], and the cc-pVTZ basis set as implemented in the GAUSSIAN03 program [24]. The electronic structure is determined by performing QMC calculations using the optimized atomic structures of the clusters from the DFT calculations. The QMC calculations are performed using the CASINO code [25] in two steps. First, we use the variational Monte Carlo (VMC) with a trial wave function of Slater-Jastrow type,

$$\Psi_T(R) = D_\uparrow(\phi_i)D_\downarrow(\phi_i)e^U, \quad (1)$$

where R is the electronic configuration, D_\uparrow and D_\downarrow are determinants of up- and down-spin orbitals, and the ϕ 's are the single-particle orbitals which are extracted from the DFT calculation. The Jastrow factor U in Eq. (1) is a sum of homogeneous, isotropic electron-electron terms $u(r_{ij}, \alpha)$, isotropic electron-core terms $\chi(r_{iI}, \beta)$ centered on the core, and isotropic electron-electron-core terms $f(r_{iI}, r_{jI}, r_{ij}, \eta)$, where $r_{ij} = r_i - r_j$, $r_{iI} = r_i - r_I$, and r_I is the position of the core I and r_i is the position of the electron i . The variational parameters α , β , and η are optimized by minimization of the energy variance.

Second, we perform the diffusion Monte Carlo (DMC) simulation to remove most of the variational bias of the VMC calculation, and consequently, the optimized trial wave function is used as a guide wave function for the importance sampling. In this method, an imaginary time operator $e^{-i\tau H}$ is used repeatedly (within the short-time approximation) to propagate the trial wave function at the long-time limit $i\tau \rightarrow \infty$. For large τ , the ground-state energy E_G is obtained. We also employ the fixed-node (FN-DMC) approximation, in which the nodes of the solution are equal to the nodes of the trial wave function; i.e., the nodes are not optimized during the simulation. For a few studied systems, we perform a series of runs with three time steps, 0.001, 0.0025, and 0.005 a.u., then, the DMC energy data are extrapolated linearly to the small time-step limit. Such a procedure has shown that the runs converge at a time step of about 0.001 a.u. This means that the difference between the extrapolated DMC value and DMC data at the time step 0.001 a.u. is smaller than the statistical error of the extrapolated value. For the production we use time steps of 0.001 a.u. which yields an acceptance ratio higher than 99.8% in an ensemble of 10 000 walkers. In the calculations of the averages, 80 000 QMC moves are considered.

The GAUSSIAN03 program [24] has also been used to calculate the HF total energies of the linear and cyclic carbon

clusters in the limit of an infinitely large complete basis set (CBS). The basis sets used in the HF extrapolation are aug-cc-pVDZ, aug-cc-pVTZ, aug-cc-pVQZ, and aug-cc-pV5Z. For the clusters that are open-shell systems with different numbers of up- and down-spin electrons, we perform the unrestricted Hartree-Fock (UHF) calculations. However, we will not make a distinction between the restricted and unrestricted HF in the discussion of the results and we just call such calculations as HF. The extrapolation is made by fitting the HF energies with an exponential $Y(x) = Y_{\text{CBS}} + A \exp(-Bx)$ or polynomial $Y(x) = Y_{\text{CBS}} - Bx^{-3}$ forms, where Y_{CBS} is the CBS limit and x the largest angular momentum included in the basis set [26]. The HF energies for the system with one and two atoms we use the exponential function, while for the clusters with number of atoms between three and ten we use the polynomial function. The χ^2 of the fit in the two forms is smaller than 3.0×10^{-6} indicating that the basis set dependence is well described by the polynomial and exponential forms given above.

III. RESULTS AND DISCUSSION

Figure 1 shows the set of low-lying energy structures obtained from the optimization using DFT with the B3LYP functional and cc-pVTZ basis set. The spin states of the clusters are singlet or triplet. We validate the low-lying energy structures by comparing the interatomic pair potentials obtained from the QMC and DFT simulations at different bond lengths. These checks have shown that the differences between DFT and QMC calculations are smaller than one tenth of an angstrom, in agreement with previous studies [14–16,19]. Such a comparison reinforces the idea that the optimized atomic structures of the clusters obtained within the DFT can be considered as those most populated in the mass spectroscopy experiment. Here the available experimental equilibrium bond length values for C_2 are 1.2429 Å and 1.3119 Å for singlet and triplet [27] states, respectively. The corresponding values obtained from our calculations are 1.2472 Å and 1.3018 Å with the differences of 0.0043 and 0.01 Å, respectively, from the experimental ones. For larger clusters there are no available experimental bond lengths. Nevertheless, our values are in good agreement with those from other theoretical approaches [28–31]. In addition, further calculations on their electronic structures have shown (in previous studies [15,16,19] and also here as we present latter in this paper) that the QMC simulations are able to approximate experimental values within the chemical accuracy such as the atomic binding energy, vertical and adiabatic detachment energy, the ionization potential energy, as well the dissociation energy, which are quantities sensitive to the atomic structure of the clusters. We provide in Table I the total energies of the clusters under investigation and all the bond lengths in the clusters with their respective labels indicated in Fig. 1.

In order to analyze the lowest-energy structures of the linear and cyclic carbon clusters, we have employed the average bond length (d_{av}) and effective coordination number (ECN). The ECN is defined differently from the traditional coordination number (CN) by attributing a different weight to the bonds based on their lengths [32,33]. For instance, the bond length smaller than d_{av} contributes with a weight larger

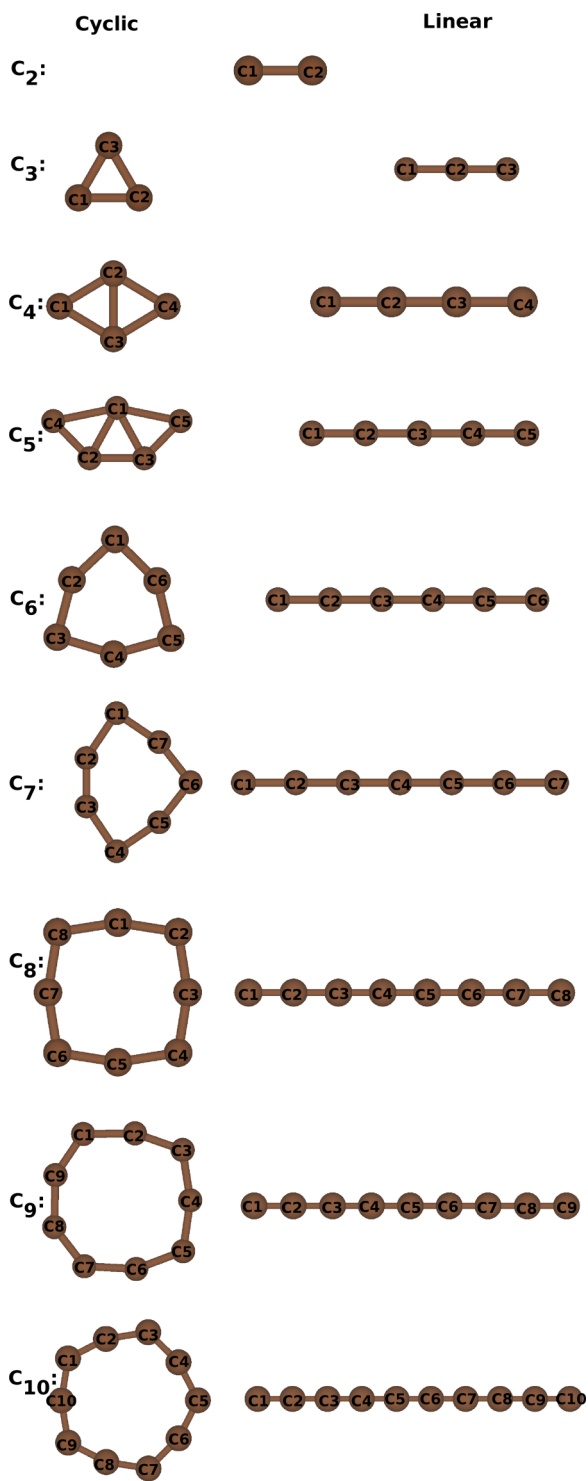


FIG. 1. The cyclic and linear structures of the C_n clusters obtained by DFT with B3LYP using the GAUSSIAN03 program. The main bond lengths are given in Table I.

than unit. Within such a definition, the ECN does not need a cutoff bond length as used in the CN. For structures of high symmetry ECN has the same value of CN. The ECN is more useful in analyzing possible structural trends and it has been applied with great success to investigate the structure of several clusters, in particular for metallic clusters [19,34,35].

TABLE I. The HF and FN-DMC total energies in a.u. and bond lengths in angstroms of the carbon clusters C_n . The spin multiplicity of the clusters is also given. Estimated statistical errors are indicated in the parentheses.

Clusters C_n	HF	FN-DMC	Spin state	Bond length (Å)
1	-37.69399	-37.8289(2)	3	
1		-37.84438(5) ^a	3	
2	-75.40698	-75.9021(3)	1	1.2472
2		-75.9229(6) ^a	1	1.2426
3 (linear)	-113.39968	-113.9984(7)	1	1.2876
3 (cyclic)	-113.37687	-113.9758(6)	3	1.3642
4 (linear)	-151.24650	-152.0220(7)	3	C_{12} : 1.3054 C_{23} : 1.2867
4 (cyclic)	-151.20606	-152.0159(5)	1	C_{12} : 1.4422 C_{23} : 1.4934
5 (linear)	-189.09211	-190.1235(3)	1	C_{12} : 1.2825 C_{23} : 1.2789
5 (cyclic)	-188.99589	-190.0344(7)	1	C_{12} : 1.4633 C_{14} : 1.6599 C_{23} : 1.3985 C_{24} : 2.5119
6 (linear)	-226.95225	-228.1555(7)	3	C_{12} : 1.2957 C_{23} : 1.2840 C_{34} : 1.2713
6 (cyclic)	-226.89641	-228.1748(8)	1	C_{12} : 1.3194
7 (linear)	-264.78316	-266.2339(9)	1	C_{12} : 1.2818 C_{23} : 1.2836 C_{34} : 1.2692
7 (cyclic)	-264.74281	-266.2271(7)	1	C_{12} : 1.3966 C_{23} : 1.2547 C_{17} : 1.3334 C_{67} : 1.3161
8 (linear)	-302.65539	-304.2850(9)	3	C_{12} : 1.2910 C_{23} : 1.2855 C_{34} : 1.2700 C_{45} : 1.2774
8 (cyclic)	-302.60206	-304.2980(8)	1	C_{12} : 1.3802 C_{81} : 1.2522
9 (linear)	-340.47637	-342.3753(9)	1	C_{12} : 1.2812 C_{23} : 1.2862 C_{34} : 1.2674 C_{45} : 1.2735
9 (cyclic)	-340.43371	-342.3654(9)	1	C_{12} : 1.3175 C_{19} : 1.2634 C_{89} : 1.3243 C_{23} : 1.2848 C_{34} : 1.2991
10 (linear)	-378.35940	-380.4165(10)	3	C_{12} : 1.2881 C_{23} : 1.2868 C_{34} : 1.2689 C_{45} : 1.2774 C_{56} : 1.2705
10 (cyclic)	-378.38462	-380.5284(10)	1	C_{12} : 1.2884 C_{23} : 1.2886

^aQMC with multideterminant expansion from Ref. [36].

The definition of the ECN and d_{av} invokes the use of the following exponential averaging functions,

$$ECN_i = \sum_j \exp \left[1 - \left(\frac{d_{ij}}{d_{av}^i} \right)^6 \right] \quad (2)$$

and

$$d_{av}^i = \frac{\sum_j d_{ij} \exp \left[1 - \left(\frac{d_{ij}}{d_{av}^i} \right)^6 \right]}{\sum_j \exp \left[1 - \left(\frac{d_{ij}}{d_{av}^i} \right)^6 \right]}, \quad (3)$$

where d_{ij} is the distance between the atom i and the atom j . The estimation of d_{av}^i is obtained self-consistently using the condition $|d_{av}^i(\text{new}) - d_{av}^i(\text{old})| < 10^{-4}$. The initial value of d_{av}^i is assumed to be the smallest bond length between the atom i and all other atoms. The converged value of d_{av}^i is used to obtain the ECN_i . The functional form of ECN described by the combination of an exponential function and the term d_{ij}/d_{av}^i raised to the sixth power in the argument of the exponential is used to obtain the ECNs as the standard CN for undistorted high-symmetry clusters and crystalline systems with simple lattices [34]. The final values of the ECN and d_{av} are obtained as averages of a particular configuration

$$ECN = \frac{1}{n} \sum_i^n ECN_i \quad (4)$$

and

$$d_{av} = \frac{1}{n} \sum_i^n d_{av}^i, \quad (5)$$

where n is the total number of atoms in the cluster or the cluster size.

Figure 2 shows the numerical simulation results of d_{av} and ECN as a function of the cluster size for both the linear and cyclic carbon clusters. The cluster size affects the average bond length d_{av} in a nontrivial way as shown in Fig. 2(a). For the cyclic clusters under investigation, their d_{av} is larger than that of the corresponding linear ones and also depends more strongly on the cluster size. This means that in the cyclic structures the nuclei are more distant from each other in comparing to the linear ones. Therefore, in the cyclic configuration the screening of the valence electrons is reduced leading to a larger repulsion between the nuclei. However, with increasing the number of atoms in the cyclic clusters, this repulsion decreases because the radius of the cluster becomes larger. Notice that in the cyclic configuration, the clusters C_4 and C_5 have different behavior from the others. The average bond lengths of the clusters C_4 and C_5 are obviously larger and their ECNs are also larger than the others. For $n \geq 6$, the cyclic clusters are of a simple ring structure and their average bond length d_{av} decreases with increasing the cluster size, tending to values of the linear ones. This is expected since in large clusters, d_{av} of different atomic configurations should tend to the same value. In Fig. 2(b) we notice that the ECN reflects sensitively the atomic structure of the clusters. The ECNs of the cyclic clusters C_4 and C_5 are larger than 2 because of their multiple-ring structures with atoms of 3 or 4 bonds. For the other cyclic clusters ($n = 3$ and $6 \leq n \leq 10$), the ECN is 2 or smaller. $ECN = 2$ for the cyclic clusters C_3

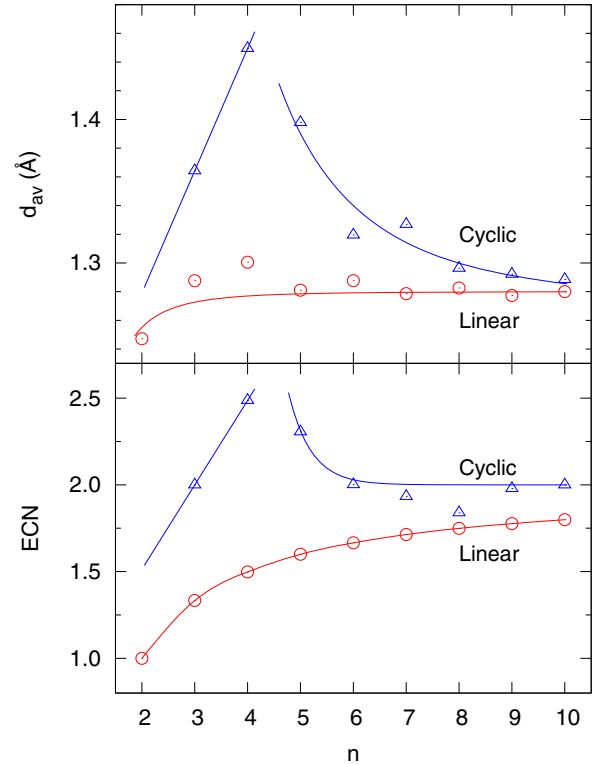


FIG. 2. The weighted average bond length (d_{av}) and effective coordination number (ECN) of the carbon clusters as a function of the cluster size. The blue triangle and red circles are calculation results for the cyclic and linear structures, respectively. The solid lines are only guides to the eyes.

and C_6 because each atom in these rings has two bonds of the same length. Variation of the bond length is responsible for $ECN < 2$ in both the linear and simple ring clusters (see Table I). This is evident in the ring clusters with $6 \leq n \leq 10$. For the ring cluster C_8 , ECN has the smallest value among the ring clusters because two very different bond lengths (about 10% difference) appear alternatively in the C_8 ring structure. For larger ring clusters such as C_9 and C_{10} , the bond lengths become more uniform and their ECN very close to 2. In the linear clusters, the ECN increases with increasing the clusters size following approximately a square-root relation. In the large linear-chain limit, the edge effect vanishes and the ECN converges to 2. This value means that an atom in the cluster always lies between two bonds of the same length.

The total energies of the clusters obtained from the DMC and HF calculations are given in Table I for the atomic structures shown in Fig. 1. The correlation energy E_{corr} is defined as the difference between the exact ground-state energy (considered to be the DMC energy E_{DMC}) and the HF energy E_{HF} within a complete basis set limit, i.e., $E_{corr} = E_{DMC} - E_{HF}$. The DMC results show for both the linear and cyclic clusters that the electron correlation lowers the total energies by about 0.5% with respect to the HF ones. In the table, we also include the QMC results for the C atom and C_2 dimer obtained with an elaborate multideterminant wave function by Morales *et al.* [36]. Their calculations with a more sophisticated multideterminant wave function improve the correlation

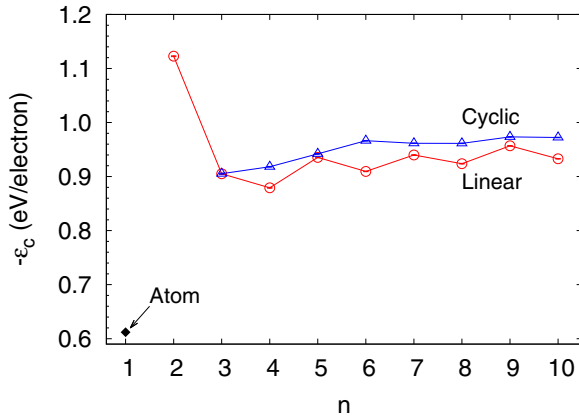


FIG. 3. The average correlation energy per electron in the clusters. The black diamond, blue triangles, and red circles are results for the carbon atom and cyclic and linear clusters, respectively.

energy. However, in comparison to their results, our QMC calculations within the single-determinant approximation take into account 90% and 96% of the correlation energy of the C atom and C₂ dimer, respectively.

In Fig. 3 we show the average correlation energy per electron ε_c in both the linear and cyclic carbon clusters as a function of the cluster size. The average correlation energy ε_c is given by E_{corr}/N , where $N = 6n$ is the number of electrons in the cluster C_n . The value of ε_c in a single carbon atom is also indicated in the figure. A noticeable difference is that the average correlation energies in a single carbon atom and a carbon dimer C₂ are very different from each other and also different from the other larger clusters with $n \geq 3$. For $3 \leq n \leq 10$, $-\varepsilon_c$ varies less than 0.1 eV/electron. But, the value of $-\varepsilon_c$ of the C₂ cluster is about 0.5 eV/electron larger than that of a single carbon atom and about 0.2 eV/electron larger than the other clusters. This reflects strong chemical bonding and electron correlation in the C₂ dimer. In the linear clusters for $n \geq 3$ the odd-number size is relatively more favorable in terms of the correlation energy than their neighbors of even-number size. The cyclic clusters do not display such pronounced even-odd oscillation as the linear ones show, but the clusters C₆ and C₉ appear to be more favorable than their neighbors in terms of the correlation. This is directly related to the second-order Jahn-Teller distortion, mainly for the cluster C₆. The values of $-\varepsilon_c$ of the cyclic clusters are larger than the linear ones for all the clusters though for C₃ and C₅ their differences are very small, being less than 0.007 eV. The explanation for the oscillatory trend for the linear clusters is that the even- and odd-number size clusters have open and closed shells, respectively. The clusters with even-number carbon atoms have two unpaired valence electrons which are, therefore, less correlated than the paired electrons in a doubly occupied orbital in the closed-shell systems. The oscillating behavior is also due to the alternation of the spin multiplicity in the cluster ground states. The odd-number size clusters are closed-shell systems with spin singlet state, whereas even-number carbon clusters are open-shell systems with spin triplet. Notice that, for the cyclic configuration, the oscillation pattern is strongly reduced due mainly to the interplay of the electron delocalization (enhanced in some

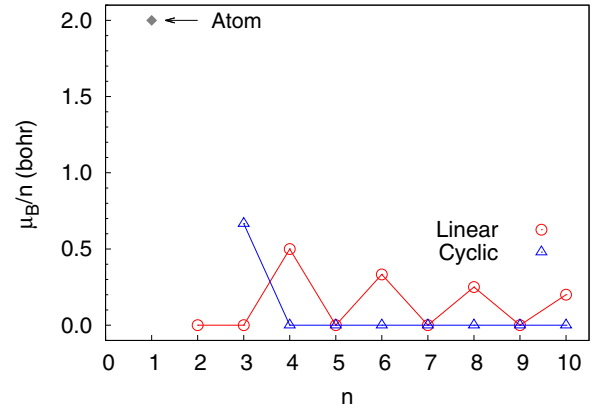


FIG. 4. Total magnetic moment per atom of the linear (red circles) and cyclic (blue triangles) clusters as a function of the cluster size. The black diamond shows the magnetic moment of a carbon atom.

cases by the aromaticity effects) and the effects of the spin state. In the present case, it is manifested by reducing the role of the spin multiplicity in these clusters.

Figure 4 shows the total magnetic moment per atom of the linear and cyclic carbon clusters as a function of the cluster size. The magnetic moment is defined as $\mu = g_s S \mu_B$, where S is the total spin angular momentum of the cluster, g_s is the g factor, and μ_B is the Bohr magneton. The spin multiplicities of the clusters are given in Table I. Notice that, differently from most metallic clusters, both the linear and cyclic carbon clusters admit only odd-spin states. Most of the cyclic clusters under investigation have zero total magnetic moment except the cluster C₃. For the clusters with the linear structure, although the ones with odd-number atoms have no net magnetic moment, the linear clusters with even-number atoms have the total magnetic moment $2\mu_B$. Due to this magnetic property the carbon chain has been proposed as transport junction between Au electrodes [11]. Magnetism found in materials containing only s and p electrons, instead of traditionally localized d or f electrons, appear to be very interesting to spintronics [10,11].

Next, we study the atomic binding energy of the clusters. The binding energy (E_b) of the cluster is given by

$$E_b = [E(C_n) - nE_a]/n, \quad (6)$$

where n is the number of atoms in the cluster, $E(C_n)$ the total energy of the carbon cluster, and E_a the energy of an isolated atom. The general trend of the binding energy per atom as shown in Fig. 5 is that the value of $-E_b$ increases with increasing the cluster size for both the cyclic and linear clusters. We also achieve a good agreement between the DMC binding energies and the available experimental results for the clusters with up to 5 atoms. The DMC binding energies for linear clusters practically match the experimental values of C₃, C₄, and C₅ from Refs. [27] and [37] with differences less than 1%. This indicates that the computationally predicted structures are very close to the experimental ones. For most of the studied clusters we found that the differences between our DFT-B3LYP and DMC binding energies are on the order of 10^{-2} eV (the only exception is the cluster C₂ for which

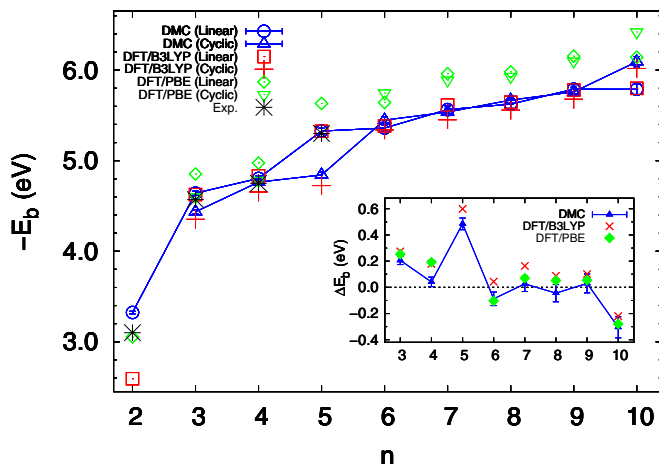


FIG. 5. The binding energy per atom of the linear and cyclic structures as a function of the cluster size n . The DMC and DFT-B3LYP results are from this work, the DFT-PBE binding energy obtained by Mauney *et al.* [38], and the experimental values from Refs. [27] and [37]. The inset shows the difference between the binding energies of the linear and cyclic clusters.

the difference is 0.73 eV). A comparison with recent DFT-PBE binding energies obtained by Mauney *et al.* [38] shows that their values follow the same trend as the DMC and experimental results, but overall with an overestimation of a few tenths of an electron volt except for C_2 . In the case of the cluster C_2 , the DFT binding energy from Ref. [38] is 0.3 eV lower than the DMC value. Furthermore, we also have performed single-point DFT-PBE calculations (not shown here) and the obtained results agree with those of Mauney *et al.* [38]. This means the differences between the DFT and DMC calculations are practically due to approximations in the xc functionals; i.e., there are no structural effects involved when comparing the binding energies obtained by Mauney *et al.* [38] with our results. The inset in Fig. 5 shows the difference between the binding energies of the linear and cyclic clusters ΔE_b . The positive (negative) value of ΔE_b indicates that the linear (cyclic) isomer is more stable. Our results indicate that the linear structures are more stable for the clusters C_3 , C_4 , C_5 , C_7 , and C_9 , and the cyclic for C_6 , C_8 , and C_{10} . However, the values of ΔE_b for $n = 4, 7, 8$, and 9 are very close to zero indicating that the linear and cyclic isomers are almost degenerate. Especially, in the cases of $n = 7$ and 9 , ΔE_b is practically zero within the error bar. On the other side, the DMC calculation shows clearly that the cyclic structures of the clusters C_6 and C_{10} are more stable. Notice that previous experimental measurements [31] indicated the linear structures for C_7 and C_9 and the cyclic for C_{10} .

The DFT-PBE calculations predict the linear ground-state structures for all studied clusters except C_6 and C_{10} being cyclic, whereas the DFT-B3LYP simulations indicate the only exception is C_{10} . In spite of the DFT-B3LYP yielding a better agreement with the DMC binding energies, it leads to a larger discrepancy in the difference of the binding energies of different isomers shown in the inset in Fig. 5, which determines the optimized ground-state structure. The noticeable differences of the DFT binding energies by using different xc

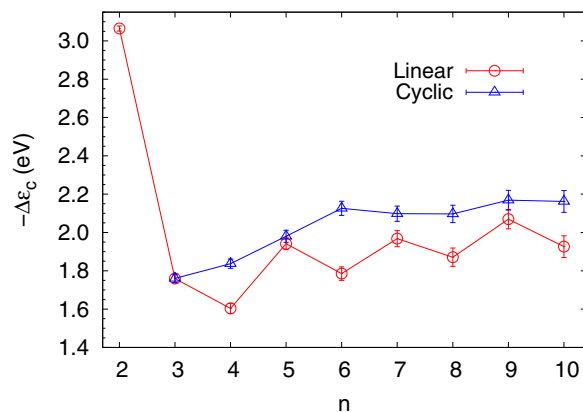


FIG. 6. The electron-correlation contribution to the binding energy per atom as a function of the cluster size n . The blue triangles and red circles are results for cyclic and linear structures, respectively.

functionals shown above as well as the discrepancies in their differences for different isomers shown in the inset in Fig. 5 may be attributed to the error cancellations presented in the DFT binding energy calculations. The comparison of different calculation results shows clearly the critical importance of the electron correlation effect and the deficiencies of DFT calculations in obtaining accurate binding energies of the carbon clusters. Therefore, an accurate method for treating xc effects such as QMC is important for understanding the electronic properties of carbon clusters.

Figure 6 shows the electron-correlation contribution to the binding energy per atom $-\Delta\epsilon_c$ as a function of the cluster size n . This quantity is obtained by $\Delta\epsilon_c = E_b^{\text{DMC}} - E_b^{\text{HF}}$, where E_b^{DMC} and E_b^{HF} are the binding energies per atom obtained from the DMC and HF calculations, respectively, defined by Eq. (6). For the linear clusters, the electron-correlation contribution exhibits odd-even oscillation, indicating that the clusters with odd-number carbon atoms are relatively more favored in terms of correlation energy than their neighbors with even-number atoms. Similar oscillation is not observed in the cyclic clusters. However, the cyclic isomers gain more correlation energy than the linear ones for all cluster sizes. As we have shown in previous studies on metal clusters [18,21], the electron correlation is crucial to determine the binding energies of the metal clusters. The present calculation shows that the carbon clusters are not different. The electron correlation has also a significant impact on the binding energies of the carbon clusters. From the difference of the binding energies obtained by the DMC and HF calculations, we find that the correlation effects are responsible for roughly 40% of the total binding energies of both the cyclic and linear clusters. For the C_2 cluster, the electron-correlation contribution represents about 50% in its binding energy. In general the impact of the electron-correlation contribution to the binding energy is greater in the cyclic isomers than in their corresponding linear ones in all the studied cases.

Finally, we will discuss the stability of the carbon clusters and try to understand better the effects of electron correlation on their stability. For this, we have calculated the dissociation energy (ΔE_n) and the second difference in energy

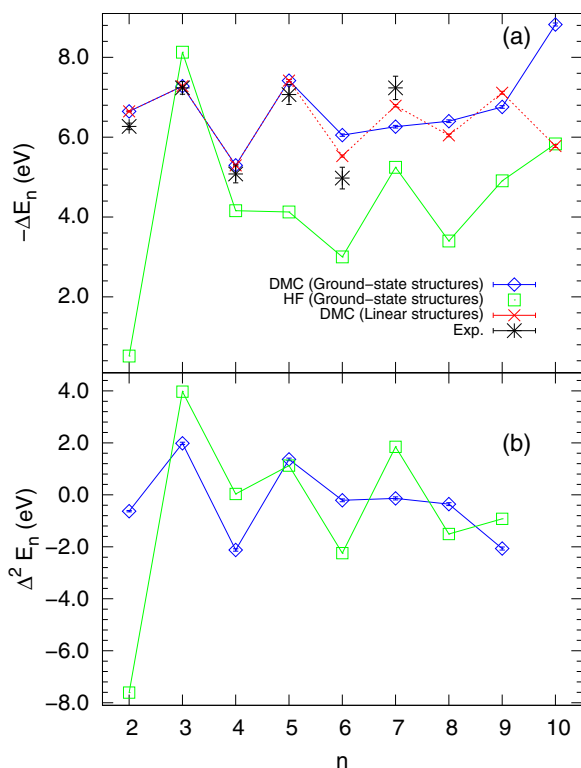


FIG. 7. (a) The dissociation energy and (b) the second difference in energy of the more stable carbon clusters as a function of the cluster size n . The blue lozenges and green squares are the DMC and HF results, respectively, with the optimized ground-state structures. In (a) the black stars show the experimental values from Ref. [39] and the red crosses indicate the DMC results within the linear structures.

($\Delta^2 E_n$) of the more stable carbon clusters using the following definitions,

$$\Delta E_n = E(C_n) - E(C_{n-1}) - E_a \quad (7)$$

and

$$\Delta^2 E_n = E(C_{n-1}) + E(C_{n+1}) - 2E(C_n). \quad (8)$$

The obtained ΔE_n and $\Delta^2 E_n$ by the DMC calculations in Fig. 7 show a pronounced odd-even alternation with the number of carbon atoms in the clusters. A comparison between the DMC and HF results shows that the electron correlation enhances the dissociation energy by up to 52% of its total values, stabilizing significantly the clusters. We also obtain a very good agreement of the DMC dissociation energies with the available experimental results [39] for $n \leq 7$ given in Fig. 7(a). The blue lozenges in the figure are the DMC dissociation energies within the optimized ground-state structures of the clusters and the red crosses for the linear ones. Since the available experimental dissociation energies are for linear structures only, a better agreement with the DMC results within the linear structures instead of the optimized ones is

observed. For the clusters with $n \leq 5$, the red crosses match the blue lozenges because the optimized ground-state structures are linear. For larger clusters, the optimized structures are cyclic for C_6 , C_8 , and C_{10} . For the second difference in energy given in Fig. 7(b), the DMC and HF results show similar oscillation behaviors for $n \leq 7$. It is well accepted as a criterion of relative stability of the clusters with a local maximum in $-\Delta E_n$ and a corresponding maximum in $\Delta^2 E_n$. Therefore, the DMC results in Fig. 7 indicate that the carbon clusters of odd-number atoms $n = 3$ and 5 with linear structures are more stable.

IV. CONCLUSIONS

In this paper, we carried out DFT, DMC, and HF calculations to study the structural and electronic properties of small carbon clusters. The lowest-energy structures for the cyclic and linear isomers were determined by DFT which also provides the single-particle orbitals to the VMC trial wave function. The ground-state energies of the carbon clusters under investigations were obtained from the DMC calculations. We estimated the electron correlation energy, the atomic binding energy, the dissociation energy, and the second difference in energy of the clusters. In general, the obtained bond lengths, the binding energies, and the dissociation energies are in very good agreement with the available experimental results. For the atomic binding energy, our DMC results reach a remarkable agreement with the experimental values obtained in Refs. [27] and [37]. A comparative analysis of the dissociation energy and the second difference in energy indicate that the linear isomers C_3 and C_5 are the most stable ones.

Through a comparison between the DMC and HF results, we also studied the electron correlation effects in the clusters. For the linear isomers, the odd-number size clusters are relatively more favored in terms of correlation energy than their neighbors of even-number size, whereas for cyclic clusters we do not observe the oscillation pattern. However, the correlation energies in the cyclic isomers are larger than those in the linear ones for all cluster sizes. The impact of electron correlation on the binding energies in the cyclic clusters varies from 35% to 40% of their values, while for the linear clusters they are about 32% to 38%. The effects of electron correlation are also essential to stabilize the clusters, enhancing by up to 52% their dissociation energy.

ACKNOWLEDGMENTS

This research was supported by the Brazilian agencies CNPq, FAPESP, and FAPEG/PRONEX under Grant No. 201710267000503. The authors thank the National Laboratory for Scientific Computing (LNCC/MCTI, Brazil) for providing computational resources of the SDumont super-computer and the Centro Nacional de Processamento de Alto Desempenho em São Paulo (CENAPAD-SP).

[1] A. V. Orden and R. J. Saykally, *Chem. Rev.* **98**, 2313 (1998).

[2] J. Hutter, H. P. Luthi, and F. Diederich, *J. Am. Chem. Soc.* **116**, 750 (1994).

- [3] G. v. Helden, M.-T. Hsu, P. R. Kemper, and M. T. Bowers, *J. Chem. Phys.* **95**, 3835 (1991).
- [4] H. Gilman, *Science* **93**, 47 (1941).
- [5] J. I. Martinez and J. A. Alonso, *Phys. Chem. Chem. Phys.* **20**, 27368 (2018).
- [6] A. I. Boldyrev and L.-S. Wang, *Chem. Rev.* **105**, 3716 (2005).
- [7] N. Tombros, S. J. van der Molen, and B. J. van Wees, *Phys. Rev. B* **73**, 233403 (2006).
- [8] N. Tombros, C. Jozsa, M. Popinciuc, H. T. Jonkman, and B. J. van Wees, *Nature (London)* **448**, 571 (2007).
- [9] V. I. Kurmashev, Y. V. Timoshkov, T. I. Orehovskaja, and V. Y. Timoshkov, *Phys. Solid State* **46**, 696 (2004).
- [10] F. Kuemmeth, S. Llani, D. C. Ralph, and P. L. McEuen, *Nature (London)* **452**, 448 (2008).
- [11] Z. Y. Li, W. Sheng, Z. Y. Ning, Z. H. Zhang, Z. Q. Yang, and H. Guo, *Phys. Rev. B* **80**, 115429 (2009).
- [12] J. C. Grossman, L. Mitas, and K. Raghavachari, *Phys. Rev. Lett.* **75**, 3870 (1995).
- [13] T. Torelli and L. Mitas, *Phys. Rev. Lett.* **85**, 1702 (2000).
- [14] P. R. C. Kent, M. D. Towler, R. J. Needs, and G. Rajagopal, *Phys. Rev. B* **62**, 15394 (2000).
- [15] C. R. Hsing, C. M. Wei, N. D. Drummond, and R. J. Needs, *Phys. Rev. B* **79**, 245401 (2009).
- [16] C. R. Hsing, P. López Ríos, R. J. Needs, and C. M. Wei, *Phys. Rev. B* **88**, 165412 (2013).
- [17] B. G. A. Brito, G.-Q. Hai, and L. Cândido, *Chem. Phys. Lett.* **586**, 108 (2013).
- [18] B. G. A. Brito, L. Cândido, J. N. Teixeira Rabelo, and G.-Q. Hai, *Chem. Phys. Lett.* **616**, 212 (2014).
- [19] L. Cândido, J. N. Teixeira Rabelo, J. L. F. da Silva, and G.-Q. Hai, *Phys. Rev. B* **85**, 245404 (2012).
- [20] B. G. A. Brito, G.-Q. Hai, J. N. Teixeira Rabelo, and L. Cândido, *Phys. Chem. Chem. Phys.* **16**, 8639 (2014).
- [21] N. L. Moreira, B. G. A. Brito, J. N. T. Rabelo, and L. Cândido, *J. Comput. Chem.* **37**, 1531 (2016).
- [22] A. D. Becke, *J. Chem. Phys.* **98**, 5648 (1993).
- [23] C. Lee, W. Yang, and R. G. Parr, *Phys. Rev. B* **37**, 785 (1988).
- [24] M. J. Frish *et al.*, GAUSSIAN03, Revision C.02, Gaussian, Inc., Wallingford, CT (2004).
- [25] R. J. Needs, M. D. Towler, N. D. Drummond, and P. L. Rios, *J. Phys.: Condens. Matter* **22**, 023201 (2010).
- [26] D. Feller, *J. Chem. Phys.* **96**, 6104 (1992); **98**, 7059 (1993).
- [27] K. P. Huber and G. Herzberg, *Molecular Spectra and Molecular Structure. IV. Constants of Diatomic Molecules* (Van Nostrand Reinhold, New York, 1979).
- [28] R. O. Jones, *J. Chem. Phys.* **110**, 5189 (1999).
- [29] A. C. Ngandjong, J. Z. Mezei, J. Mougento, A. Michau, K. Hassouni, G. Lombardi, M. Seydou, and F. Maurel, *Comput. Theor. Chem.* **1102**, 105 (2017).
- [30] K. Raghavachari and J. S. Binkley, *J. Chem. Phys.* **87**, 2191 (1987).
- [31] L. Belau, S. E. Wheeler, B. W. Ticknor, M. Ahmed, S. R. Leone, W. D. Allen, H. F. Shaefer III, and M. A. Duncan, *J. Am. Chem. Soc.* **129**, 10229 (2007).
- [32] R. Hoppe, *Angew. Chem. Int. Ed. Engl.* **9**, 25 (1970).
- [33] R. Hoppe, *Z. Kristallogr.* **150**, 23 (1979).
- [34] M. J. Piotrowski, P. Piquini, and J. L. F. Da Silva, *Phys. Rev. B* **81**, 155446 (2010).
- [35] B. G. A. Brito, G.-Q. Hai, and L. Cândido, *J. Chem. Phys.* **146**, 174306 (2017).
- [36] M. A. Morales, J. McMinis, B. K. Clark, J. Kim, and G. E. Scuseria, *J. Chem. Theory Comput.* **8**, 2181 (2012).
- [37] J. Drowart, R. P. Burns, G. De Maria, and M. G. Inghram, *J. Chem. Phys.* **31**, 1131 (1959).
- [38] C. Mauney, M. B. Nardelli, and D. Lazzati, *Astrophys. J.* **800**, 30 (2015).
- [39] K. A. Gingerich, H. C. Finkbeiner, and R. W. Schmude Jr., *J. Am. Chem. Soc.* **116**, 3884 (1994).